Report

Cell Reports

A Combination of Two Human Monoclonal Antibodies Prevents Zika Virus Escape Mutations in Non-human Primates

Graphical Abstract

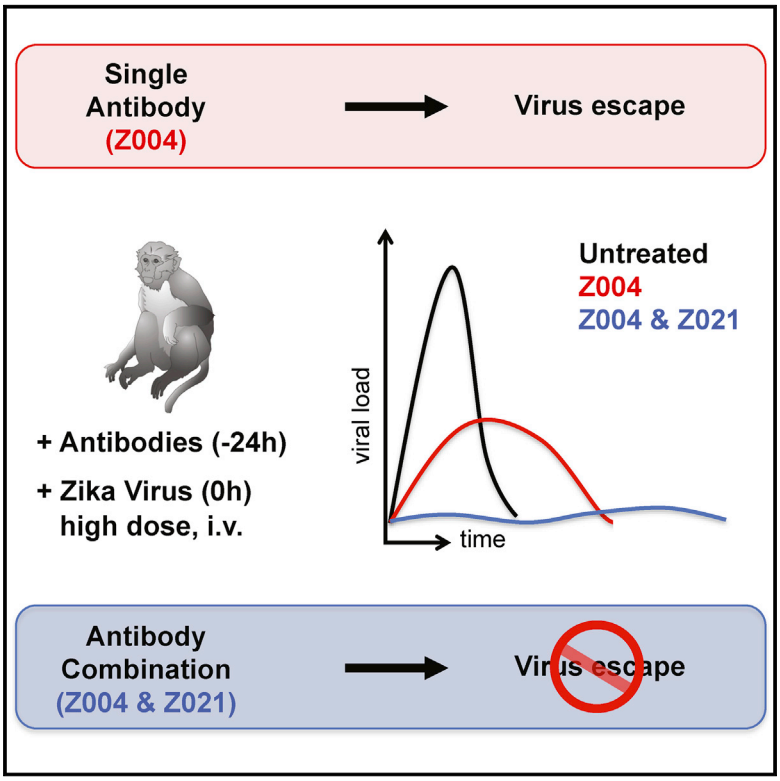

Highlights

- Monoclonal antibodies are tested in macaques challenged with high-dose Zika virus
- A single monoclonal antibody selects for Zika virus escape mutants
- A combination of two antibodies suppresses viremia and prevents escape mutants
- Antibodies engineered to avoid enhancement confer similar levels of protection

Authors

Jennifer R. Keeffe,
Koen K.A. Van Rompay,
Priscilla C. Olsen, ..., Pamela J. Bjorkman,
Michel C. Nussenzweig,
Davide F. Robbiani

Correspondence

nussen@rockefeller.edu (M.C.N.),
drobbiani@rockefeller.edu (D.F.R.)

In Brief

Passive administration of anti-Zika human monoclonal antibodies could be an efficacious and safe alternative to vaccines for at-risk populations. Keeffe et al. show that administration of a combination of two monoclonal antibodies to macaques followed by high-dose intravenous Zika challenge reduces viremia and prevents the emergence of viral escape mutations.

Keeffe et al., 2018, Cell Reports *25*, 1385–1394
November 6, 2018
https://doi.org/10.1016/j.celrep.2018.10.031

CellPress

Cell Reports
Report

A Combination of Two Human Monoclonal Antibodies Prevents Zika Virus Escape Mutations in Non-human Primates

Jennifer R. Keeffe,[1,10] Koen K.A. Van Rompay,[2,9,10] Priscilla C. Olsen,[3,7] Qiao Wang,[8] Anna Gazumyan,[3] Stephanie A. Azzopardi,[4] Dennis Schaefer-Babajew,[3] Yu E. Lee,[1] Jackson B. Stuart,[9] Anil Singapuri,[9] Jennifer Watanabe,[2] Jodie Usachenko,[2] Amir Ardeshir,[2] Mohsan Saeed,[4] Marianna Agudelo,[3] Thomas Eisenreich,[3] Stylianos Bournazos,[5] Thiago Y. Oliveira,[3] Charles M. Rice,[4] Lark L. Coffey,[9] Margaret R. MacDonald,[4] Pamela J. Bjorkman,[1] Michel C. Nussenzweig,[3,6,*] and Davide F. Robbiani[3,11,*]

[1]Division of Biology and Biological Engineering, California Institute of Technology, Pasadena, CA 91125, USA
[2]California National Primate Research Center, University of California, Davis, Davis, CA 95616, USA
[3]Laboratory of Molecular Immunology, The Rockefeller University, New York, NY 10065, USA
[4]Laboratory of Virology and Infectious Disease, The Rockefeller University, New York, NY 10065, USA
[5]Laboratory of Molecular Genetics and Immunology, The Rockefeller University, New York, NY 10065, USA
[6]Howard Hughes Medical Institute, The Rockefeller University, New York, NY 10065, USA
[7]Faculdade de Farmácia, Universidade Federal do Rio de Janeiro, Rio de Janeiro 21941-901, Brazil
[8]Key Laboratory of Medical Molecular Virology of MOE/MOH, School of Basic Medical Sciences, Shanghai Medical College of Fudan University, Shanghai 200032, China
[9]Department of Pathology, Microbiology and Immunology, School of Veterinary Medicine, University of California, Davis, Davis, CA 95616, USA
[10]These authors contributed equally
[11]Lead Contact
*Correspondence: nussen@rockefeller.edu (M.C.N.), drobbiani@rockefeller.edu (D.F.R.)
https://doi.org/10.1016/j.celrep.2018.10.031

SUMMARY

Zika virus (ZIKV) causes severe neurologic complications and fetal aberrations. Vaccine development is hindered by potential safety concerns due to antibody cross-reactivity with dengue virus and the possibility of disease enhancement. In contrast, passive administration of anti-ZIKV antibodies engineered to prevent enhancement may be safe and effective. Here, we report on human monoclonal antibody Z021, a potent neutralizer that recognizes an epitope on the lateral ridge of the envelope domain III (EDIII) of ZIKV and is protective against ZIKV in mice. When administered to macaques undergoing a high-dose ZIKV challenge, a single anti-EDIII antibody selected for resistant variants. Co-administration of two antibodies, Z004 and Z021, which target distinct sites on EDIII, was associated with a delay and a 3- to 4-log decrease in peak viremia. Moreover, the combination of these antibodies engineered to avoid enhancement prevented viral escape due to mutation in macaques, a natural host for ZIKV.

INTRODUCTION

Zika virus (ZIKV) is a member of the *Flavivirus* genus, which includes four serotypes of dengue virus (DENV1–4), West Nile virus (WNV), yellow fever virus (YFV), and other vector-borne viruses that cause human morbidity and mortality (Weaver and Reisen, 2010). ZIKV causes mild symptoms consisting of fever, headache, rash, conjunctivitis, and arthralgia in an estimated 20% of infected individuals. In addition, infection is occasionally associated with severe neurologic problems that require hospitalization, such as meningoencephalitis or the immune-mediated Guillain-Barré syndrome (Miner and Diamond, 2017; Muñoz et al., 2016). The most severe consequences of infection are manifest in fetuses, which can develop devastating developmental aberrations, including microcephaly, collectively referred to as congenital Zika syndrome (Brasil et al., 2016; Del Campo et al., 2017). Infection of macaques, a natural host of ZIKV, during pregnancy frequently leads to fetal demise (Dudley et al., 2018), and in some non-human primate models, prenatal and early postnatal infection is associated with fetal and infant neuropathology and persistent functional and behavioral abnormalities (Coffey et al., 2018; Mavigner et al., 2018).

There are no approved treatments for ZIKV. Vaccines for ZIKV are under development, but the path to approval may be exceedingly difficult because of antibody cross-reactivity with other flaviviruses and the possibility of disease enhancement (Bardina et al., 2017; George et al., 2017; Halstead, 2018; Harrison, 2016; Heinz and Stiasny, 2017; Katzelnick et al., 2017; Salje et al., 2018; Stettler et al., 2016). Passive administration of monoclonal antibodies represents an alternative approach to vaccines because human monoclonal antibodies can effectively neutralize the virus *in vitro* and protect against ZIKV infection in mice (Fernandez et al., 2017; Robbiani et al., 2017; Sapparapu et al., 2016; Stettler et al., 2016; Swanstrom et al., 2016; Yu et al., 2017). In addition, antibodies can be engineered to prevent interaction with Fcγ receptors that mediate enhancement and

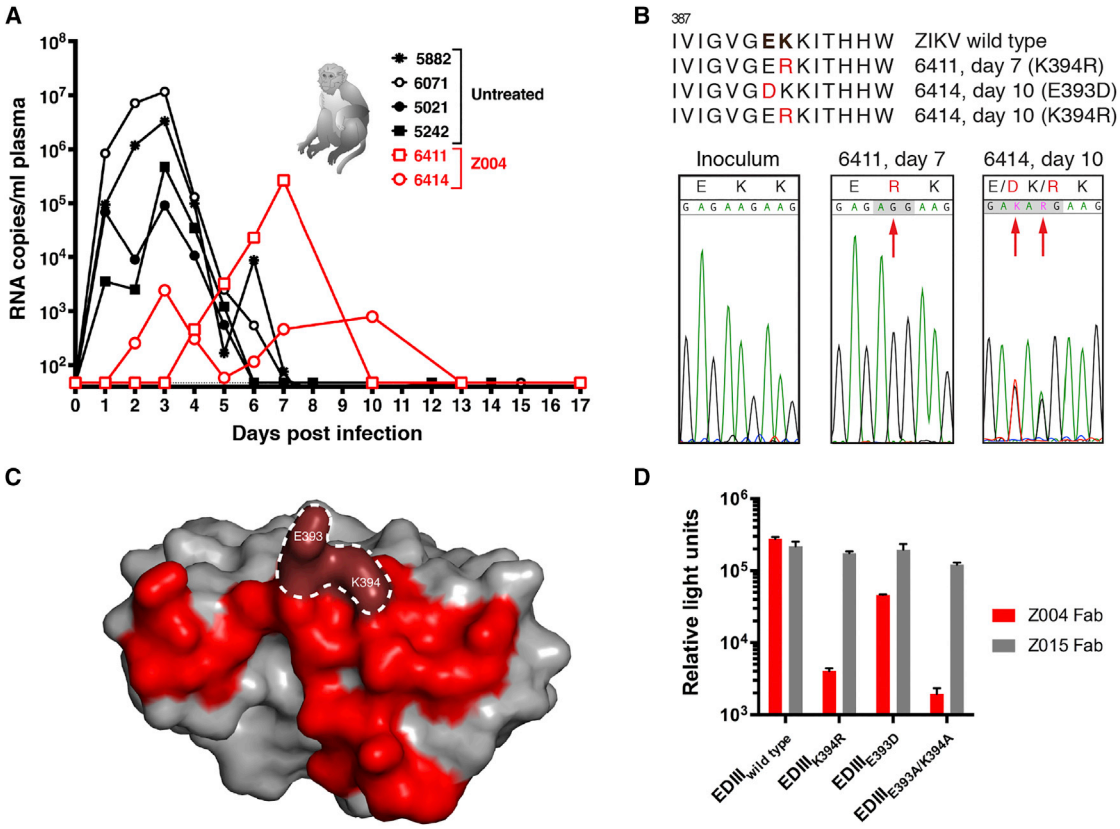

Figure 1. Administration of Z004 Alone Leads to the Emergence of Resistant ZIKV in Rhesus Macaques (*Macaca mulatta*)

(A) Macaques were administered monoclonal antibody Z004 (red) 1 day before intravenous inoculation with 10^5 PFU of ZIKV or were untreated (black). The graph shows plasma viral RNA levels of ZIKV over time as determined by qRT-PCR.

(B) ZIKV mutations emerging in macaques treated with Z004 alone. An alignment in the region of residues E393-K394 (bold) within the EDIII is shown at the top, and chromatograms of the PCR amplicons showing the mutations (indicated by red arrows) are shown at the bottom. Amino acid changes compared to the inoculum sequence are highlighted in red. In macaque 6414, E393D and K394R are on separate viral RNAs, as determined by sequencing of the cloned amplicon.

(C) The epitope of ZIKV EDIII recognized by the Z004-related antibody Z006 is shown in red (PDB: 5VIG). The E393-K394 residues are highlighted.

(D) Impaired binding of Z004 to the EDIII escape mutants. ELISA demonstrates reduced binding of Z004 Fab to $EDIII_{K394R}$ and $EDIII_{E393D}$. The positive control antibody Z015 recognizes an epitope that is independent of the E393 and K394 residues. Data are presented as mean ± SD of triplicates, and a representative of two experiments is shown.

See also Figure S1.

thus minimize the risk of disease enhancement (Beltramello et al., 2010).

A combination of three antibodies targeting epitopes on the ZIKV envelope domain II and III regions was recently shown to be effective at preventing viremia in macaques (Magnani et al., 2017b), although the same three antibodies in combination failed to prevent virus transmission to the fetus (Magnani et al., 2018). Moreover, it was reported that a single antibody to a conformational epitope prevents ZIKV viremia for 7 days after low-dose challenge (Abbink et al., 2018), but viremia was not evaluated for longer periods of time or upon high-dose viral challenge.

Here, we investigate the efficacy of the potent anti-envelope domain III (EDIII) antibody Z004 (Robbiani et al., 2017) against high-dose viral challenge in macaques over an extended time period, as well as molecularly characterize a second human anti-EDIII monoclonal antibody, Z021, and examine its protective activity in combination with Z004.

RESULTS

Z004 is one of several human monoclonal antibodies that were isolated from an individual with high levels of serum neutralizing activity against ZIKV (Robbiani et al., 2017). Z004 has strong activity against ZIKV and DENV1 *in vitro* and protects *Ifnar1*$^{-/-}$ mice from lethal ZIKV challenge (Robbiani et al., 2017). To determine whether Z004 is efficacious against ZIKV in primates, we administered it to rhesus macaques 24 hr before high-dose intravenous challenge (10^5 plaque forming units [PFUs]) with a Brazilian strain of ZIKV. Infection was monitored by qRT-PCR to detect viral RNA in the plasma (Figure 1A). All four control animals developed viremia, which peaked on day 3, with plasma viral loads ranging from 10^5 to 10^7 RNA copies/mL (Figure 1A, black). In controls, viremia cleared spontaneously beginning on day 6 (Figure 1A; Coffey et al., 2017). In contrast, the Z004-treated macaques showed delayed and prolonged viremia, with viral loads

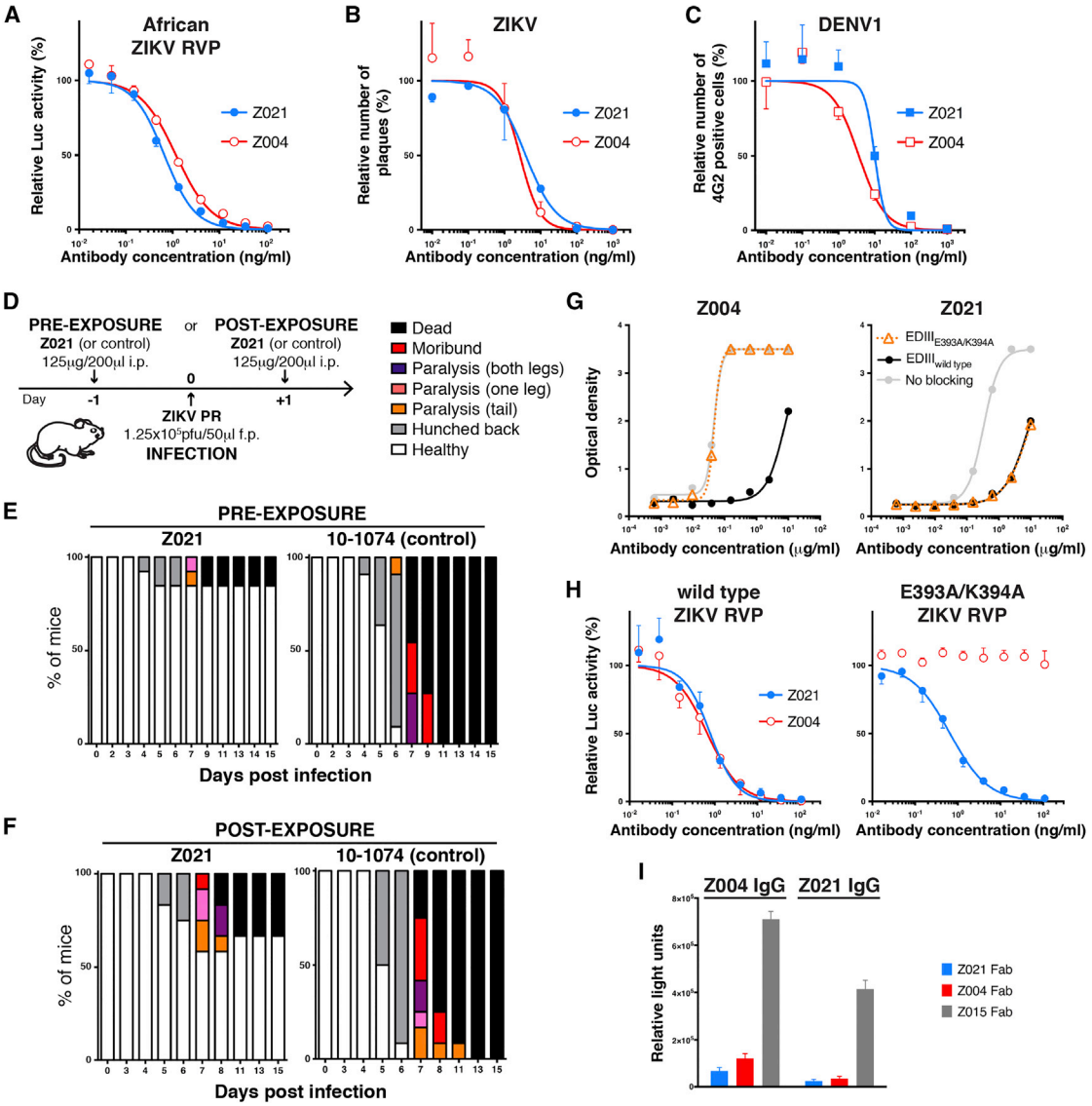

Figure 2. Z021 Neutralizes ZIKV and Recognizes a Different Epitope than Z004

(A) Z021 neutralizes ZIKV RVPs corresponding to the African strain. Neutralization by Z004 is shown alongside for comparison. Data are presented as mean ± SD of triplicates.

(B) Z021 is effective against ZIKV *in vitro*. ZIKV neutralization was determined by measuring the ability of increasing concentrations of Z021 to reduce the number of plaques in a PRNT assay. Data are presented as mean ± SD of two independent experiments.

(C) Z021 is effective against DENV1 *in vitro*. DENV1 neutralization was assessed by measuring the relative number of 4G2-positive infected cells by flow cytometry. Data are presented as mean ± SD of triplicates.

(A–C) Values are relative to control antibody 10-1074. Antibody Z004 is shown alongside for comparison (Robbiani et al., 2017). A representative of two independent experiments is shown.

(D–F) Z021 protects mice from ZIKV disease. Layout of the experiment (D). *Ifnar1*$^{-/-}$ mice were treated with Z021 or control 10-1074 antibody 1 day before (E) or 1 day after (F) challenge with ZIKV in the footpad (f.p.). Mice were monitored for symptoms and survival. The graph indicates death or symptoms. Survival: $p < 0.0001$ (pre-exposure) and $p = 0.0002$ (post-exposure). Symptoms: $p = 0.0002$ (pre-exposure) and $p = 0.0006$ (post-exposure; Mantel-Cox test). The number of mice used in pre-exposure experiments was 13 (Z021) and 11 (10-1074); for post-exposure experiments, 12 animals were used in each group. Data represent two combined experiments.

(G) Residues E393-K394 of ZIKV EDIII are not required for Z021 binding. Graphs show ELISA binding to ZIKV EDIII by increasing concentrations of antibody Z004 (left) or Z021 (right) after blocking with wild-type EDIII or $EDIII_{E393A/K394A}$.

(H) Residues E393-K394 are not required for ZIKV neutralization by Z021. Graphs show neutralization of ZIKV luciferase RVPs by Z021 and Z004 using wild-type RVPs (left) or RVPs mutated at the Z004-binding site (E393A-K394A; right). Data are presented as mean ± SD of triplicates, and a representative of two experiments is plotted. Values are relative to no antibody control.

(legend continued on next page)

reaching only 3×10^3 to 5×10^5 RNA copies/mL (Figure 1A, red). Thus, Z004 alone alters the course of ZIKV infection and leads to decreased but prolonged viremia.

To determine whether the viremia in Z004-treated animals was associated with viral escape mutations, we sequenced the antibody target region EDIII of the virus recovered from the plasma of the treated macaques on days 7 and 10. In both animals, the circulating viruses contained mutations in the EDIII (K394R in one animal and E393D or K394R in the other) (Figures 1B and 1C). Viruses encoding mutations were not observed in the untreated controls or in the inoculum (data not shown). While D393 is present in ZIKV strains of African origin, R394 has not been reported in the Virus Pathogen Resource database (ViPR; May 24, 2018). ELISA assays using ZIKV $EDIII_{E393D}$ and $EDIII_{K394R}$ mutant proteins confirmed that these mutations interfere with Z004 binding (Figure 1D). In contrast to the macaques, antibody resistance mutations were rare in *Ifnar1*$^{-/-}$ mice treated with Z004; nevertheless, the only mouse in a cohort of eight that developed mutations had the same K394R substitution observed in macaques (Figure S1). We conclude that high-dose intravenous ZIKV challenge in the presence of a single monoclonal antibody, Z004, leads to selection of resistant viral mutants.

Z021 is another human monoclonal antibody that, like Z004, was isolated from an individual with exceptionally high serum neutralizing activity against ZIKV (Robbiani et al., 2017). Z021 binds to the EDIII of both ZIKV and DENV1, neutralizes ZIKV reporter viral particles (RVPs) bearing Asian/American or African lineage E proteins with a half maximal inhibitory concentration (IC_{50}) of 1 ng/mL and 0.7 ng/mL, respectively (Figure 2A; Robbiani et al., 2017), and has strong activity in plaque reduction neutralization test (PRNT) using an infectious Puerto Rican strain of ZIKV (IC_{50} of 4 ng/mL; Figure 2B). Like Z004, Z021 is also a potent neutralizer of DENV1 (IC_{50} of 10.1 ng/mL; Figure 2C).

To determine whether Z021 is effective against ZIKV *in vivo*, we administered Z021 to *Ifnar1*$^{-/-}$ mice either 24 hr before or 24 hr after ZIKV challenge (Figure 2D). Whereas all control mice developed symptoms and died (n = 11, Figure 2E), only 15% succumbed to infection when Z021 was administered before infection (n = 13; p = 0.0002 for disease and p < 0.0001 for survival; Figure 2E). Moreover, only 42% developed symptoms and 33% succumbed to disease when the antibody was administered 1 day after infection (n = 12; p = 0.0006 for disease and p = 0.0002 for survival; Figure 2F). We conclude that Z021 is efficacious against ZIKV *in vitro* and protects *Ifnar1*$^{-/-}$ mice against lethal challenge.

Z004 binding to and neutralization of ZIKV and DENV1 is critically dependent on ZIKV EDIII residue K394 and also partially dependent on E393 (DENV1 residues K385 and E384, respectively; Figure 1D; Robbiani et al., 2017). To determine whether Z004 and Z021 recognize distinct neutralizing epitopes on EDIII, we performed antigen competition ELISA assays (Figure 2G; see STAR Methods). Each monoclonal antibody was incubated with saturating amounts of either wild-type ZIKV EDIII or an EDIII bearing mutations in the Z004 target site that interfere with its binding and neutralizing activity ($EDIII_{E393A/K394A}$; Figure 1D; Robbiani et al., 2017). Residual binding to wild-type EDIII was then measured by ELISA. Whereas Z004 binding to ZIKV was only blocked by wild-type ZIKV, binding of Z021 was blocked by both wild-type and ZIKV $EDIII_{E393A/K394A}$, indicating that residues E393 and K394 are critical for Z004, but not required for Z021 binding (Figure 2G). In agreement with this finding, Z004 failed to neutralize ZIKV RVPs that were altered to bear the E393A/K394A mutations while Z021 remained potent against the mutant RVPs *in vitro* (Figure 2H). To determine whether the Z004 and Z021 epitopes overlap, we performed antibody competition ELISA assays, which showed that the antigen-binding fragment (Fab) of Z021 did not bind to ZIKV EDIII immobilized by Z004 immunoglobulin G (IgG), and vice versa (Figure 2I; see STAR Methods). Thus, Z021 recognizes a neutralizing epitope on the EDIII that does not require E393-K394 but that is nearby or overlapping the epitope recognized by Z004.

To gain insight into how Z021 recognizes the Zika and dengue envelope proteins, we solved crystal structures of Z021 in complex with the EDIII of ZIKV and of DENV1 (Figure 3; Tables S1 and S2) and compared them to the previously obtained structures of the Z006 and Z004 antibodies in complex with the same viral antigens (Robbiani et al., 2017). Z021 recognizes the lateral ridge of ZIKV and DENV1 EDIII and binds to both antigens in a similar orientation (Figure 3A). Although it recognizes the lateral ridge region of EDIII, Z021 does not bind to the same epitope as Z004 or the related Z006 but instead recognizes a distinct but overlapping epitope. When compared to Z004 (when bound to DENV1 EDIII) or Z006 (when bound to ZIKV EDIII), the Z021 Fab is rotated ~45° around an axis near the complementarity determining region 2 (CDRH2), positioning the heavy chains in similar regions, while the light chains exhibit divergent footprints (Figure 3B). Z021 makes heavy- and light-chain contact to the EDI-EDIII hinge region (the N-terminal end of the EDIII construct), the BC loop, and the DE loop of ZIKV EDIII, and heavy chain contacts to the FG loop. Notably, Z021 does not contact $E393_{ZIKV}$ or $K394_{ZIKV}$, consistent with the biochemical data indicating that these residues are not required for Z021 activity (Figure 2). When compared to Z006, Z021 makes additional contacts to the EDI-EDIII hinge region and DE loops of ZIKV EDIII (Figure 3C). Thus, consistent with the ELISA and neutralization results (Figure 2), Z021 and Z004 recognize distinct but overlapping epitopes on EDIII.

To determine the efficacy of the combination of Z004 and Z021 against high-dose intravenous challenge with ZIKV, we co-administered the two antibodies to macaques 24 hr before infection. All three macaques developed delayed infections with low levels of viremia that peaked at 10^2–10^3 RNA copies/mL (Figures 4A and 4B). In contrast to macaques treated with

(I) Z004 and Z021 antigen-binding fragments (Fabs) cannot bind to ZIKV EDIII simultaneously. ZIKV EDIII antigen was immobilized in an ELISA with either Z004 IgG (left) or Z021 IgG (right) and then incubated with a His-tagged Fab of Z021, Z004, or Z015. Fab binding to the IgG-immobilized ZIKV EDIII was detected by anti-His secondary antibody. The positive control Z015 Fab recognizes an epitope that is distinct from that of both Z021 and Z004 (Robbiani et al., 2017). Data are presented as mean ± SD of quadruplicates and are representative of two experiments.

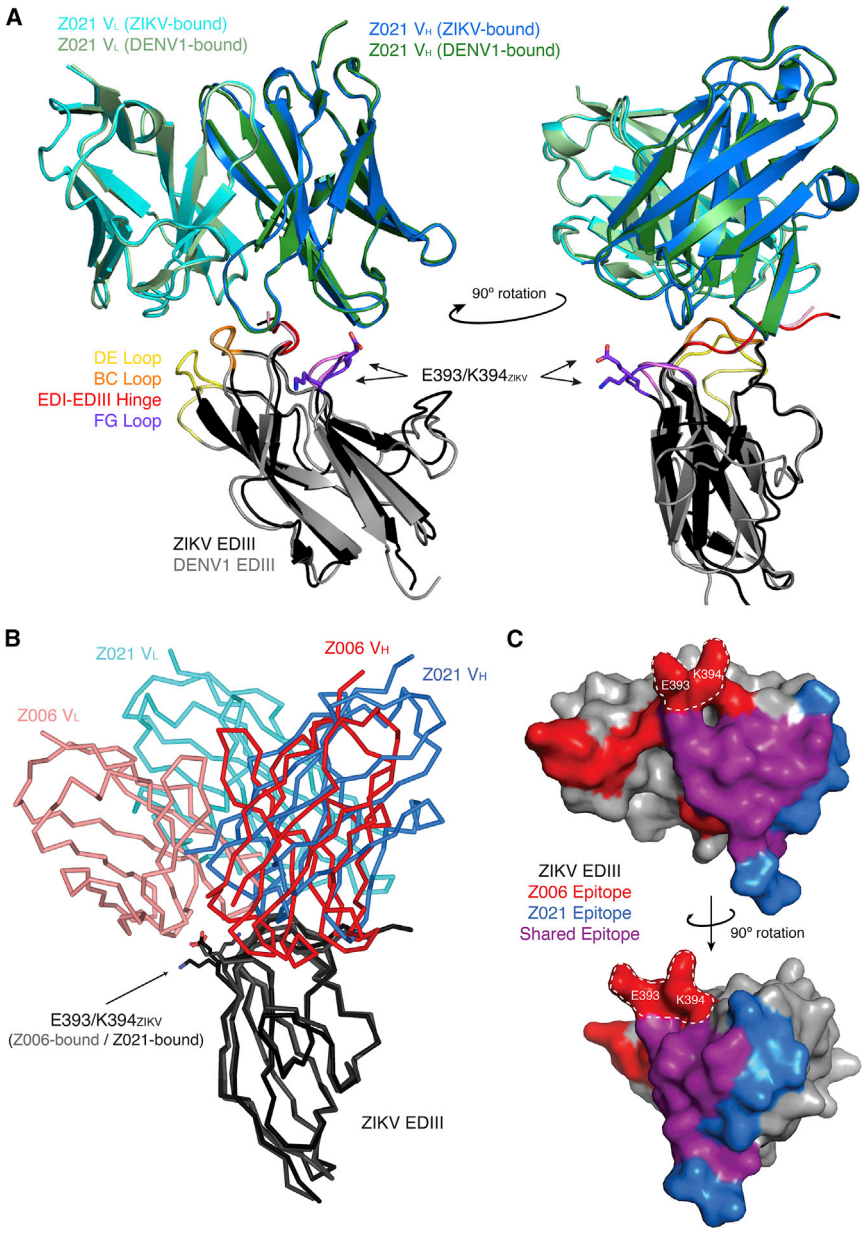

Figure 3. Comparison of Z021 and the Z004-Related Antibody, Z006, Binding to the ZIKV and DENV1 EDIII Domain

(A) Superimposition of the Z021 Fab-ZIKV complex with the Z021 Fab-DENV1 complex. The EDI-EDIII hinge region and loops of the ZIKV EDIII (bright colors) and DENV1 EDIII (light colors) within the epitope are highlighted, and the side chains of E394 and K395 residues of ZIKV are shown in sticks. The two views are related by a 90° rotation.

(B) Superimposition of Z021 Fab-ZIKV EDIII complex with Z006 Fab-ZIKV EDIII complex (PDB: 5VIG). The V_HV_L of Z021 Fab is rotated ~45° around an axis near CDRH2 compared to the Z006 V_HV_L bound to the same antigen.

(C) The epitopes of Z021 and Z006 on ZIKV EDIII are overlapping but distinct. EDIII residues within 4 Å of Z021 Fab (blue), Z006 Fab (red), or both (purple) are highlighted on a surface representation of the ZIKV EDIII from the Z021-ZIKV EDIII complex structure. The E393-$K394_{ZIKV}$ motif is outlined. The two views are related by a 90° rotation.

See also Tables S1 and S2.

Z004 alone (Figure 1), there were no mutations in the EDIII target site of the two antibodies (data not shown).

Late occurrence of viremia in some animals was not a consequence of rapid clearance of Z004 and Z021, since high levels of human antibodies were detectable in the macaque plasma (Figure S2). Similar results were obtained with Z004 and Z021 Fc mutant antibodies (GRLR) that are unable to mediate enhancement but maintain antiviral efficacy *in vitro* and in mice (Figures S3 and S4): peak viral loads were comparable between wild-type and GRLR treated macaques (brown and green bars in Figure 4B) and no EDIII mutations were detected in either group. Although a trend for delayed peak viremia was observed in the macaques receiving the combination of wild-type antibodies (mean of 11 days versus 4 days in macaques receiving GRLR antibodies), this difference is not statistically significant ($p = 0.2$; Figure 4A). Notably, in contrast to the macaques that received Z004 + Z021, plasma from macaques treated with Z004+Z021 (GRLR) antibodies did not enhance infection *in vitro* (Figure 4C). A K294R mutation, which is outside of the EDIII region targeted by the antibodies, was detected in one of the emerging viruses; however, RVPs containing K294R remained sensitive to both Z004 and Z021, suggesting that this is not a resistance mutation (Figure S4D). Thus, treatment of non-human primates with the combination of Z004 and Z021, two antibodies that target distinct but overlapping epitopes on the EDIII lateral ridge, suppresses and delays viremia in macaques infected intravenously with a high dose of ZIKV. Moreover, the combination of two antibodies prevents the emergence of ZIKV escape variants. Finally, antibodies whose Fc region is engineered to prevent enhancement provide similar levels of protection as antibodies with a wild-type Fc region.

DISCUSSION

We have determined the molecular mechanism of antigen binding by Z021 (this work) and Z004 (Robbiani et al., 2017), two potent neutralizing monoclonal antibodies against ZIKV and DENV1, and established that in combination, they prevent viral escape mutations in non-human primates.

It has been difficult to develop vaccines against the four DENV serotypes because of the complications associated with disease

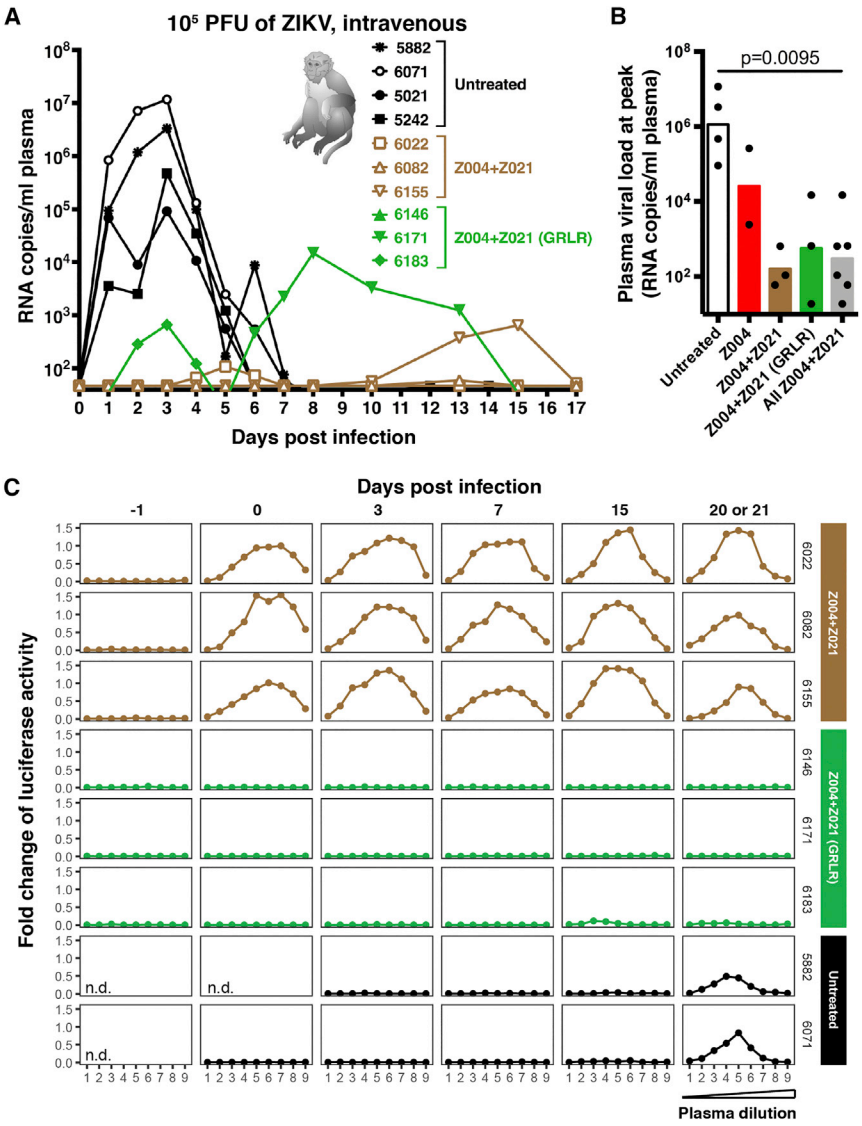

Figure 4. The Combination of Z004 and Z021 Antibodies Protects ZIKV-Challenged Macaques

(A) Macaques were administered a combination of Z004 and Z021 (brown) or a combination of the same antibodies containing mutations in the Fc that prevent Fcγ receptor binding (Z004-GRLR and Z021-GRLR; green) 1 day before intravenous inoculation with 10^5 PFU of ZIKV. The graph shows plasma viral RNA levels of ZIKV over time as determined by qRT-PCR. Untreated controls are the same as in Figure 1.

(B) Peak viral RNA loads in plasma are decreased by antibody treatment (based on Figures 1A and 4A). The p value was determined with the Mann-Whitney test. The gray bar represents the peak viral load of both Z004 + Z021 and Z004 + Z021 (GRLR) groups combined.

(C) Plasma of macaques treated with the combination of Z004-GRLR and Z021-GRLR fails to induce antibody-dependent enhancement (ADE) of infection in K-562 cells by ZIKV RVPs. Dilutions of macaque plasma (1:50–1:328,050; 9 dilutions in total) obtained at different time points were assayed for the ability to induce ZIKV RVP infection (see STAR Methods). n.d., not determined due to lack of plasma sample.

See also Figures S2–S4.

enhancement by cross-reactive antibodies (de Silva and Harris, 2018; Halstead, 2018; Screaton and Mongkolsapaya, 2018; Whitehead and Subbarao, 2018). ZIKV antibodies can cross-react with DENV and cause DENV enhancement in animal models. Therefore, it is anticipated that developing safe and effective ZIKV vaccines may be challenging (Andrade and Harris, 2018; George et al., 2017; Stettler et al., 2016).

Moreover, flaviviruses are RNA viruses that undergo high rates of error-prone replication, producing mutant variants that can be selected for resistance (Diamond, 2003; Drake et al., 1998; Elena et al., 2000). Indeed, resistant viral variants arise in antibody-containing cell cultures infected with DENV (Lin et al., 1994; Lok et al., 2001; Zou et al., 2012), WNV (Beasley and Barrett, 2002; Chambers et al., 1998), YFV (Daffis et al., 2005), Japanese encephalitis virus (Shimoda et al., 2013), tick-borne encephalitis virus (Holzmann et al., 1989), and ZIKV (Wang et al., 2017a). Resistance to monoclonal antibodies has also been documented in mice challenged with WNV (Sapkal et al., 2011) and rhesus macaques challenged with high doses of DENV (Lai et al., 2007; Magnani et al., 2017a). Our experiments are consistent with these earlier observations and extend them to ZIKV in non-human primates by showing that administration of a single antibody leads to the selection of resistant viruses.

To test the hypothesis that two antibodies might be more effective than one, we molecularly characterized Z021. Structural analysis of Z021 and comparison to Z004 (and related Z006) revealed that the two antibodies target overlapping but distinct sites. Z021 contacts the EDI-EDIII hinge region of ZIKV and DENV1 EDIII with both its heavy and light chains, while Z004 and Z006 make more extensive contacts to the FG loop, including the E393-K394$_{ZIKV}$ motif (E384-K385$_{DENV1}$). Because the E393-K394$_{ZIKV}$ motif is peripheral to the Z021 epitope, viruses with mutations at these positions are likely to remain sensitive to Z021. These differences probably account for the efficacy of this combination of two antibodies despite the similarities in their target sites.

In high-dose challenge experiments, the combination of two monoclonal antibodies further decreased peak viremia compared to Z004 alone (Figure 4B). The antiviral effects of the antibodies were independent of their ability to bind to Fcγ receptors or to enhance infection *in vitro*. However, in contrast to prophylaxis with Z004 alone, where resistant variants were detected in both treated animals, there were no viral escape mutants in

any of the six macaques treated with the combination of Z004 and Z021. Thus, the combination of these two antibodies is advantageous over Z004 alone due to their ability to prevent viral escape.

Z004 and Z021 target the EDIII lateral ridge, which is one of the key sites of viral attachment to cells, and both block infection *in vitro*. However, they do not provide sterile protection, despite high levels in circulation. One potential explanation for the disparity between *in vitro* and *in vivo* results is that ZIKV can attach to and infect cells through a number of different receptors, some of which may not be present in the Huh-7.5 cells used to measure infectivity *in vitro* (Heinz and Stiasny, 2017; Miner and Diamond, 2017). For example, virus attachment and entry via these receptors could be mediated through epitopes outside of the EDIII lateral ridge targeted by Z004 and Z021. Finally, viremia was delayed in 5 of the 8 treated macaques; an intriguing hypothesis is that during this time, ZIKV resides in and replicates in immune-privileged sites such as brain and testes that cannot be reached by antibodies (Iwasaki, 2017; Mital et al., 2011).

Our results differ from experiments where a single monoclonal was protective against low-dose subcutaneous ZIKV challenge (Abbink et al., 2018). The difference may be due to a 100-fold higher infectious dose of ZIKV delivered intravenously in our experiments. An additional possibility is that the animals in the low-dose experiments were only monitored for 7 days, which may not have been sufficient to document delayed infection seen after antibody treatment (Abbink et al., 2018). Whether other antibodies, single or in combination, will be completely protective after high-dose challenge remains to be determined but would be highly relevant for further clinical development, since the precise dose delivered by the *Aedes aegypti* vector is not known (Abbink et al., 2018; Magnani et al., 2017b).

Antibodies induced by vaccination or infection with any one of the DENV serotypes may fail to neutralize a second serotype and instead enhance dengue disease, with potentially catastrophic consequences. It is possible that dengue enhancement would also be mediated by cross-reactive antibodies elicited by vaccination against ZIKV (Andrade and Harris, 2018; George et al., 2017; Stettler et al., 2016). Because of this uncertainty, passive antibody administration for protection against ZIKV may represent a safe and practical alternative to vaccination during pregnancy and for infants and travelers, since antibodies can be engineered to prevent enhancement and have greatly extended half-lives by incorporating known Fc mutations (Gautam et al., 2018; Griffin et al., 2017; Ko et al., 2014; Robbie et al., 2013; Zalevsky et al., 2010) (https://www.clinicaltrials.gov identifier NCT02878330). Our observations indicate that a combination of two antibodies targeting the EDIII lateral ridge is not sufficient for complete protection of high-dose ZIKV challenge, and combinations of additional antibodies are likely required.

STAR★METHODS

Detailed methods are provided in the online version of this paper and include the following:

- KEY RESOURCES TABLE
- CONTACT FOR REAGENT AND RESOURCE SHARING
- EXPERIMENTAL MODEL AND SUBJECT DETAILS
  - Macaques
  - Mice
  - Cell lines
  - Viruses
- METHOD DETAILS
  - Production of antibodies and Fabs
  - Production of ZIKV proteins
  - Generation and production of RVPs
  - *In vitro* neutralization and ADE assays
  - ELISA assays
  - Surface plasmon resonance
  - Processing of macaque blood samples
  - Isolation and quantitation of viral RNA
  - Virus sequencing
  - Crystallization and structure determination
- QUANTIFICATION AND STATISTICAL ANALYSIS
- DATA AND SOFTWARE AVAILABILITY

SUPPLEMENTAL INFORMATION

Supplemental Information includes four figures and three tables and can be found with this article online at https://doi.org/10.1016/j.celrep.2018.10.031.

ACKNOWLEDGMENTS

We thank Kai-Hui Yao, Daniel Yost, and Jovana Golijanin at Rockefeller, as well as the veterinary staff, pathology staff, and the staff of Colony Management and Research Services and Clinical Laboratory at the California National Primate Center for expert assistance. We thank Alisa Voll, Tiffany Luong, and the Caltech Protein Expression Center directed by Dr. Jost Vielmetter for cloning and expression and purification of proteins and Anthony P. West, Jr., Harry B. Gristick, Beth Stadtmueller, and Christopher Barnes for help with crystallographic methods and helpful discussions. We also thank Jens Kaiser from the Molecular Observatory at the Beckman Institute at the California Institute of Technology, Ruslan Sanishvili at APS beamline 23-ID-D (Argonne National Laboratory), and the staff at beamline 12–2, Stanford Synchrotron Radiation Lightsource (SSRL), for their assistance with crystallographic data collection and processing. Operations at SSRL are supported by the US Department of Energy and NIH, and operations at APS are supported by the NIH (NIGMS and National Cancer Institute). This work was supported by the NIH (pilot awards U19AI111825 and UL1TR001866 to D.F.R.; grants R01AI037526, UM1AI100663, U19AI111825, P01AI138938, and UL1TR001866 to M.C.N.), funding by Lyda Hill (to M.C.N.), NIH grants R01AI124690 and U19AI057229 (CCHI pilot project), The Rockefeller University Development Office and anonymous donors (C.M.R. and M.R.M.), the Office of Research Infrastructure Programs/OD (grant P51OD011107), start-up funds from the Pathology, Microbiology and Immunology Department (to L.L.C.), NIH grant 1R21AI129479-01 (to K.K.A.V.R.), and the Molecular Observatory at Caltech supported by the Gordon and Betty Moore Foundation (P.J.B.). Support was also provided by the Robertson Therapeutic Development Fund (D.F.R. and M.C.N.). P.C.O. is supported by the Pew Latin American Fellows Program in the Biomedical Sciences, D.S.-B. is supported by Studienstiftung des deutschen Volkes, and M.C.N. is an HHMI Investigator.

AUTHOR CONTRIBUTIONS

J.R.K. performed biochemical experiments, solved and analyzed crystal structures, and wrote structure-related parts of the paper together with P.J.B. P.C.O., Q.W., A.G., D.-S.B., M.A., S.A.A., M.S., Y.E.L., and T.E. produced reagents, developed protocols, and conducted immunology, virology, and mouse infection experiments. S.B. performed the SPR assays. T.Y.O. analyzed data, including statistical analysis. A.S. and J.B.S. conducted qRT-PCR and sequencing experiments from macaques under

supervision of L.L.C., who also edited the manuscript. J.W., J.U., and A.A. performed macaque experiments under the supervision of K.K.A.V.R., who also edited the manuscript. C.M.R. and M.R.M. supervised, interpreted experimental results, and edited the manuscript. M.C.N. supervised, designed, and interpreted experiments and wrote the paper. D.F.R. designed, supervised, and conducted experiments, interpreted experimental results, and wrote the paper.

DECLARATION OF INTERESTS

D.F.R., M.C.N., and the Rockefeller University have filed a patent application for antibodies Z004 and Z021.

Received: August 9, 2018
Revised: September 15, 2018
Accepted: October 5, 2018
Published: November 6, 2018

REFERENCES

Abbink, P., Larocca, R.A., Dejnirattisai, W., Peterson, R., Nkolola, J.P., Borducchi, E.N., Supasa, P., Mongkolsapaya, J., Screaton, G.R., and Barouch, D.H. (2018). Therapeutic and protective efficacy of a dengue antibody against Zika infection in rhesus monkeys. Nat. Med. *24*, 721–723.

Adams, P.D., Afonine, P.V., Bunkóczi, G., Chen, V.B., Davis, I.W., Echols, N., Headd, J.J., Hung, L.W., Kapral, G.J., Grosse-Kunstleve, R.W., et al. (2010). PHENIX: a comprehensive Python-based system for macromolecular structure solution. Acta Crystallogr. D Biol. Crystallogr. *66*, 213–221.

Andrade, D.V., and Harris, E. (2018). Recent advances in understanding the adaptive immune response to Zika virus and the effect of previous flavivirus exposure. Virus Res. *254*, 27–33.

Bardina, S.V., Bunduc, P., Tripathi, S., Duehr, J., Frere, J.J., Brown, J.A., Nachbagauer, R., Foster, G.A., Krysztof, D., Tortorella, D., et al. (2017). Enhancement of Zika virus pathogenesis by preexisting antiflavivirus immunity. Science *356*, 175–180.

Battye, T.G., Kontogiannis, L., Johnson, O., Powell, H.R., and Leslie, A.G. (2011). iMOSFLM: a new graphical interface for diffraction-image processing with MOSFLM. Acta Crystallogr. D Biol. Crystallogr. *67*, 271–281.

Beasley, D.W., and Barrett, A.D. (2002). Identification of neutralizing epitopes within structural domain III of the West Nile virus envelope protein. J. Virol. *76*, 13097–13100.

Beltramello, M., Williams, K.L., Simmons, C.P., Macagno, A., Simonelli, L., Quyen, N.T., Sukupolvi-Petty, S., Navarro-Sanchez, E., Young, P.R., de Silva, A.M., et al. (2010). The human immune response to Dengue virus is dominated by highly cross-reactive antibodies endowed with neutralizing and enhancing activity. Cell Host Microbe *8*, 271–283.

Blight, K.J., McKeating, J.A., and Rice, C.M. (2002). Highly permissive cell lines for subgenomic and genomic hepatitis C virus RNA replication. J. Virol. *76*, 13001–13014.

Brasil, P., Pereira, J.P., Jr., Moreira, M.E., Ribeiro Nogueira, R.M., Damasceno, L., Wakimoto, M., Rabello, R.S., Valderramos, S.G., Halai, U.A., Salles, T.S., et al. (2016). Zika virus infection in pregnant women in Rio de Janeiro. N. Engl. J. Med. *375*, 2321–2334.

Chambers, T.J., Halevy, M., Nestorowicz, A., Rice, C.M., and Lustig, S. (1998). West Nile virus envelope proteins: nucleotide sequence analysis of strains differing in mouse neuroinvasiveness. J. Gen. Virol. *79*, 2375–2380.

Chapgier, A., Boisson-Dupuis, S., Jouanguy, E., Vogt, G., Feinberg, J., Prochnicka-Chalufour, A., Casrouge, A., Yang, K., Soudais, C., Fieschi, C., et al. (2006). Novel STAT1 alleles in otherwise healthy patients with mycobacterial disease. PLoS Genet. *2*, e131.

Coffey, L.L., Pesavento, P.A., Keesler, R.I., Singapuri, A., Watanabe, J., Watanabe, R., Yee, J., Bliss-Moreau, E., Cruzen, C., Christe, K.L., et al. (2017). Zika virus tissue and blood compartmentalization in acute infection of rhesus macaques. PLoS ONE *12*, e0171148.

Coffey, L.L., Keesler, R.I., Pesavento, P.A., Woolard, K., Singapuri, A., Watanabe, J., Cruzen, C., Christe, K.L., Usachenko, J., Yee, J., et al. (2018). Intraamniotic Zika virus inoculation of pregnant rhesus macaques produces fetal neurologic disease. Nat. Commun. *9*, 2414.

Daffis, S., Kontermann, R.E., Korimbocus, J., Zeller, H., Klenk, H.D., and Ter Meulen, J. (2005). Antibody responses against wild-type yellow fever virus and the 17D vaccine strain: characterization with human monoclonal antibody fragments and neutralization escape variants. Virology *337*, 262–272.

de Silva, A.M., and Harris, E. (2018). Which dengue vaccine approach is the most promising, and should we be concerned about enhanced disease after vaccination? The path to a dengue vaccine: learning from human natural dengue infection studies and vaccine trials. Cold Spring Harb. Perspect. Biol. *10*, a029371.

Del Campo, M., Feitosa, I.M., Ribeiro, E.M., Horovitz, D.D., Pessoa, A.L., França, G.V., García-Alix, A., Doriqui, M.J., Wanderley, H.Y., Sanseverino, M.V., et al.; Zika Embryopathy Task Force-Brazilian Society of Medical Genetics ZETF-SBGM (2017). The phenotypic spectrum of congenital Zika syndrome. Am. J. Med. Genet. A. *173*, 841–857.

Diamond, M.S. (2003). Evasion of innate and adaptive immunity by flaviviruses. Immunol. Cell Biol. *81*, 196–206.

Drake, J.W., Charlesworth, B., Charlesworth, D., and Crow, J.F. (1998). Rates of spontaneous mutation. Genetics *148*, 1667–1686.

Dudley, D.M., Van Rompay, K.K., Coffey, L.L., Ardeshir, A., Keesler, R.I., Bliss-Moreau, E., Grigsby, P.L., Steinbach, R.J., Hirsch, A.J., MacAllister, R.P., et al. (2018). Miscarriage and stillbirth following maternal Zika virus infection in nonhuman primates. Nat. Med. *24*, 1104–1107.

Elena, S.F., Miralles, R., Cuevas, J.M., Turner, P.E., and Moya, A. (2000). The two faces of mutation: extinction and adaptation in RNA viruses. IUBMB Life *49*, 5–9.

Emsley, P., and Cowtan, K. (2004). Coot: model-building tools for molecular graphics. Acta Crystallogr. D Biol. Crystallogr. *60*, 2126–2132.

Fernandez, E., Dejnirattisai, W., Cao, B., Scheaffer, S.M., Supasa, P., Wongwiwat, W., Esakky, P., Drury, A., Mongkolsapaya, J., Moley, K.H., et al. (2017). Human antibodies to the dengue virus E-dimer epitope have therapeutic activity against Zika virus infection. Nat. Immunol. *18*, 1261–1269.

Gautam, R., Nishimura, Y., Gaughan, N., Gazumyan, A., Schoofs, T., Buckler-White, A., Seaman, M.S., Swihart, B.J., Follmann, D.A., Nussenzweig, M.C., and Martin, M.A. (2018). A single injection of crystallizable fragment domain-modified antibodies elicits durable protection from SHIV infection. Nat. Med. *24*, 610–616.

George, J., Valiant, W.G., Mattapallil, M.J., Walker, M., Huang, Y.S., Vanlandingham, D.L., Misamore, J., Greenhouse, J., Weiss, D.E., Verthelyi, D., et al. (2017). Prior exposure to Zika virus significantly enhances peak dengue-2 viremia in rhesus macaques. Sci. Rep. *7*, 10498.

Griffin, M.P., Khan, A.A., Esser, M.T., Jensen, K., Takas, T., Kankam, M.K., Villafana, T., and Dubovsky, F. (2017). Safety, tolerability, and pharmacokinetics of MEDI8897, the respiratory syncytial virus prefusion F-targeting monoclonal antibody with an extended half-life, in healthy adults. Antimicrob. Agents Chemother. *61*, e01714-16.

Halstead, S.B. (2018). Which dengue vaccine approach is the most promising, and should we be concerned about enhanced disease after vaccination? There is only one true winner. Cold Spring Harb. Perspect. Biol. *10*, a030700.

Harrison, S.C. (2016). Immunogenic cross-talk between dengue and Zika viruses. Nat. Immunol. *17*, 1010–1012.

Heinz, F.X., and Stiasny, K. (2017). The antigenic structure of Zika virus and its relation to other flaviviruses: implications for infection and immunoprophylaxis. Microbiol. Mol. Biol. Rev. *81*, e00055-16.

Holzmann, H., Mandl, C.W., Guirakhoo, F., Heinz, F.X., and Kunz, C. (1989). Characterization of antigenic variants of tick-borne encephalitis virus selected with neutralizing monoclonal antibodies. J. Gen. Virol. *70*, 219–222.

Horton, H.M., Bernett, M.J., Pong, E., Peipp, M., Karki, S., Chu, S.Y., Richards, J.O., Vostiar, I., Joyce, P.F., Repp, R., et al. (2008). Potent in vitro and in vivo activity of an Fc-engineered anti-CD19 monoclonal antibody against lymphoma and leukemia. Cancer Res. *68*, 8049–8057.

Iwasaki, A. (2017). Immune regulation of antibody access to neuronal tissues. Trends Mol. Med. *23*, 227–245.

Katzelnick, L.C., Gresh, L., Halloran, M.E., Mercado, J.C., Kuan, G., Gordon, A., Balmaseda, A., and Harris, E. (2017). Antibody-dependent enhancement of severe dengue disease in humans. Science *358*, 929–932.

Ko, S.Y., Pegu, A., Rudicell, R.S., Yang, Z.Y., Joyce, M.G., Chen, X., Wang, K., Bao, S., Kraemer, T.D., Rath, T., et al. (2014). Enhanced neonatal Fc receptor function improves protection against primate SHIV infection. Nature *514*, 642–645.

Lai, C.J., Goncalvez, A.P., Men, R., Wernly, C., Donau, O., Engle, R.E., and Purcell, R.H. (2007). Epitope determinants of a chimpanzee dengue virus type 4 (DENV-4)-neutralizing antibody and protection against DENV-4 challenge in mice and rhesus monkeys by passively transferred humanized antibody. J. Virol. *81*, 12766–12774.

Lanciotti, R.S., Kosoy, O.L., Laven, J.J., Velez, J.O., Lambert, A.J., Johnson, A.J., Stanfield, S.M., and Duffy, M.R. (2008). Genetic and serologic properties of Zika virus associated with an epidemic, Yap State, Micronesia, 2007. Emerg. Infect. Dis. *14*, 1232–1239.

Lanciotti, R.S., Lambert, A.J., Holodniy, M., Saavedra, S., and Signor, Ldel.C. (2016). Phylogeny of Zika Virus in Western Hemisphere, 2015. Emerg. Infect. Dis. *22*, 933–935.

Li, T., DiLillo, D.J., Bournazos, S., Giddens, J.P., Ravetch, J.V., and Wang, L.X. (2017). Modulating IgG effector function by Fc glycan engineering. Proc. Natl. Acad. Sci. USA *114*, 3485–3490.

Lin, B., Parrish, C.R., Murray, J.M., and Wright, P.J. (1994). Localization of a neutralizing epitope on the envelope protein of dengue virus type 2. Virology *202*, 885–890.

Lok, S.M., Ng, M.L., and Aaskov, J. (2001). Amino acid and phenotypic changes in dengue 2 virus associated with escape from neutralisation by IgM antibody. J. Med. Virol. *65*, 315–323.

Lu, C.L., Murakowski, D.K., Bournazos, S., Schoofs, T., Sarkar, D., Halper-Stromberg, A., Horwitz, J.A., Nogueira, L., Golijanin, J., Gazumyan, A., et al. (2016). Enhanced clearance of HIV-1-infected cells by broadly neutralizing antibodies against HIV-1 in vivo. Science *352*, 1001–1004.

Magnani, D.M., Ricciardi, M.J., Bailey, V.K., Gutman, M.J., Pedreno-Lopez, N., Silveira, C.G.T., Maxwell, H.S., Domingues, A., Gonzalez-Nieto, L., Su, Q., et al. (2017a). Dengue virus evades AAV-mediated neutralizing antibody prophylaxis in rhesus monkeys. Mol. Ther. *25*, 2323–2331.

Magnani, D.M., Rogers, T.F., Beutler, N., Ricciardi, M.J., Bailey, V.K., Gonzalez-Nieto, L., Briney, B., Sok, D., Le, K., Strubel, A., et al. (2017b). Neutralizing human monoclonal antibodies prevent Zika virus infection in macaques. Sci. Transl. Med. *9*, eaan8184.

Magnani, D.M., Rogers, T.F., Maness, N.J., Grubaugh, N.D., Beutler, N., Bailey, V.K., Gonzalez-Nieto, L., Gutman, M.J., Pedreño-Lopez, N., Kwal, J.M., et al. (2018). Fetal demise and failed antibody therapy during Zika virus infection of pregnant macaques. Nat. Commun. *9*, 1624.

Mavigner, M., Raper, J., Kovacs-Balint, Z., Gumber, S., O'Neal, J.T., Bhaumik, S.K., Zhang, X., Habib, J., Mattingly, C., McDonald, C.E., et al. (2018). Postnatal Zika virus infection is associated with persistent abnormalities in brain structure, function, and behavior in infant macaques. Sci. Transl. Med. *10*, eaao6975.

Miner, J.J., and Diamond, M.S. (2017). Zika virus pathogenesis and tissue tropism. Cell Host Microbe *21*, 134–142.

Mital, P., Hinton, B.T., and Dufour, J.M. (2011). The blood-testis and blood-epididymis barriers are more than just their tight junctions. Biol. Reprod. *84*, 851–858.

Mouquet, H., Scharf, L., Euler, Z., Liu, Y., Eden, C., Scheid, J.F., Halper-Stromberg, A., Gnanapragasam, P.N., Spencer, D.I., Seaman, M.S., et al. (2012). Complex-type N-glycan recognition by potent broadly neutralizing HIV antibodies. Proc. Natl. Acad. Sci. USA *109*, E3268–E3277.

Muñoz, L.S., Barreras, P., and Pardo, C.A. (2016). Zika virus-associated neurological disease in the adult: Guillain-Barré syndrome, encephalitis, and myelitis. Semin. Reprod. Med. *34*, 273–279.

Pierson, T.C., Sánchez, M.D., Puffer, B.A., Ahmed, A.A., Geiss, B.J., Valentine, L.E., Altamura, L.A., Diamond, M.S., and Doms, R.W. (2006). A rapid and quantitative assay for measuring antibody-mediated neutralization of West Nile virus infection. Virology *346*, 53–65.

Robbiani, D.F., Bozzacco, L., Keeffe, J.R., Khouri, R., Olsen, P.C., Gazumyan, A., Schaefer-Babajew, D., Avila-Rios, S., Nogueira, L., Patel, R., et al. (2017). Recurrent potent human neutralizing antibodies to Zika virus in Brazil and Mexico. Cell *169*, 597–609.e511.

Robbie, G.J., Criste, R., Dall'acqua, W.F., Jensen, K., Patel, N.K., Losonsky, G.A., and Griffin, M.P. (2013). A novel investigational Fc-modified humanized monoclonal antibody, motavizumab-YTE, has an extended half-life in healthy adults. Antimicrob. Agents Chemother. *57*, 6147–6153.

Salje, H., Cummings, D.A.T., Rodriguez-Barraquer, I., Katzelnick, L.C., Lessler, J., Klungthong, C., Thaisomboonsuk, B., Nisalak, A., Weg, A., Ellison, D., et al. (2018). Reconstruction of antibody dynamics and infection histories to evaluate dengue risk. Nature *557*, 719–723.

Sapkal, G.N., Harini, S., Ayachit, V.M., Fulmali, P.V., Mahamuni, S.A., Bondre, V.P., and Gore, M.M. (2011). Neutralization escape variant of West Nile virus associated with altered peripheral pathogenicity and differential cytokine profile. Virus Res. *158*, 130–139.

Sapparapu, G., Fernandez, E., Kose, N., Bin Cao, Fox, J.M., Bombardi, R.G., Zhao, H., Nelson, C.A., Bryan, A.L., Barnes, T., et al. (2016). Neutralizing human antibodies prevent Zika virus replication and fetal disease in mice. Nature *540*, 443–447.

Screaton, G., and Mongkolsapaya, J. (2018). Which dengue vaccine approach is the most promising, and should we be concerned about enhanced disease after vaccination? The challenges of a dengue vaccine. Cold Spring Harb. Perspect. Biol. *10*, a029520.

Shimoda, H., Mahmoud, H.Y., Noguchi, K., Terada, Y., Takasaki, T., Shimojima, M., and Maeda, K. (2013). Production and characterization of monoclonal antibodies to Japanese encephalitis virus. J. Vet. Med. Sci. *75*, 1077–1080.

Stettler, K., Beltramello, M., Espinosa, D.A., Graham, V., Cassotta, A., Bianchi, S., Vanzetta, F., Minola, A., Jaconi, S., Mele, F., et al. (2016). Specificity, cross-reactivity, and function of antibodies elicited by Zika virus infection. Science *353*, 823–826.

Swanstrom, J.A., Plante, J.A., Plante, K.S., Young, E.F., McGowan, E., Gallichotte, E.N., Widman, D.G., Heise, M.T., de Silva, A.M., and Baric, R.S. (2016). Dengue virus envelope dimer epitope monoclonal antibodies isolated from dengue patients are protective against Zika virus. MBio *7*, e01123-16.

Tiller, T., Meffre, E., Yurasov, S., Tsuiji, M., Nussenzweig, M.C., and Wardemann, H. (2008). Efficient generation of monoclonal antibodies from single human B cells by single cell RT-PCR and expression vector cloning. J. Immunol. Methods *329*, 112–124.

Wang, J., Bardelli, M., Espinosa, D.A., Pedotti, M., Ng, T.S., Bianchi, S., Simonelli, L., Lim, E.X.Y., Foglierini, M., Zatta, F., et al. (2017a). A human bi-specific antibody against Zika virus with high therapeutic potential. Cell *171*, 229–241.e215.

Wang, T.T., Sewatanon, J., Memoli, M.J., Wrammert, J., Bournazos, S., Bhaumik, S.K., Pinsky, B.A., Chokephaibulkit, K., Onlamoon, N., Pattanapanyasat, K., et al. (2017b). IgG antibodies to dengue enhanced for FcγRIIIA binding determine disease severity. Science *355*, 395–398.

Weaver, S.C., and Reisen, W.K. (2010). Present and future arboviral threats. Antiviral Res. *85*, 328–345.

West, A.P., Jr., Scharf, L., Horwitz, J., Klein, F., Nussenzweig, M.C., and Bjorkman, P.J. (2013). Computational analysis of anti-HIV-1 antibody neutralization panel data to identify potential functional epitope residues. Proc. Natl. Acad. Sci. USA *110*, 10598–10603.

Whitehead, S.S., and Subbarao, K. (2018). Which dengue vaccine approach is the most promising, and should we be concerned about enhanced disease after vaccination? The risks of incomplete immunity to dengue virus revealed by vaccination. Cold Spring Harb. Perspect. Biol. *10*, a028811.

Winn, M.D., Ballard, C.C., Cowtan, K.D., Dodson, E.J., Emsley, P., Evans, P.R., Keegan, R.M., Krissinel, E.B., Leslie, A.G., McCoy, A., et al. (2011). Overview of the CCP4 suite and current developments. Acta Crystallogr. D Biol. Crystallogr. *67*, 235–242.

Yu, L., Wang, R., Gao, F., Li, M., Liu, J., Wang, J., Hong, W., Zhao, L., Wen, Y., Yin, C., et al. (2017). Delineating antibody recognition against Zika virus during natural infection. JCI Insight *2*, 93042.

Zalevsky, J., Chamberlain, A.K., Horton, H.M., Karki, S., Leung, I.W., Sproule, T.J., Lazar, G.A., Roopenian, D.C., and Desjarlais, J.R. (2010). Enhanced antibody half-life improves in vivo activity. Nat. Biotechnol. *28*, 157–159.

Zou, G., Kukkaro, P., Lok, S.M., Ng, J.K., Tan, G.K., Hanson, B.J., Alonso, S., MacAry, P.A., and Shi, P.Y. (2012). Resistance analysis of an antibody that selectively inhibits dengue virus serotype-1. Antiviral Res. *95*, 216–223.

STAR★METHODS

KEY RESOURCES TABLE

REAGENT or RESOURCE	SOURCE	IDENTIFIER
Antibodies		
Human recombinant 10-1074	Mouquet et al., 2012	N/A
Human recombinant Z004	Robbiani et al., 2017	N/A
Human recombinant Z021	Robbiani et al., 2017	N/A
Human recombinant Z015	Robbiani et al., 2017	N/A
Mouse anti-flavivirus group antigen, clone D1-4G2-4-15 (4G2)	Millipore	Cat#MAB10216; RRID:AB_827205
Goat anti-human IgG, HRP-conjugated	Jackson ImmunoResearch	Cat#109-035-098; RRID:AB_2337586
Goat anti-human IgG, HRP-conjugated	GenScript	Cat#A00166
Donkey anti-goat IgG, biotin-conjugated	Jackson ImmunoResearch	Cat#705-065-147; RRID:AB_2340397
THE His Tag Antibody	GenScript	Cat#A00186; RRID:AB_914704
Goat anti-mouse IgG, HRP-conjugated	Jackson ImmunoResearch	Cat#115-035-003; RRID:AB_10015289
Llama anti-human IgG (Captureselect)	ThermoScientific	Cat#7103322100
F(ab')2 Fragment Goat anti-human IgG, HRP-conjugated	Jackson ImmunoResearch	Cat#109-036-088; RRID:AB_2337594
Bacterial and Virus Strains		
E. coli BL21(DE3)	New England Biolabs	Cat#C2527H
Brazilian ZIKV	Laboratory of M. Busch	SPH2015
Puerto Rican ZIKV	CDC	PRVABC59
DENV1 PUO-359	Laboratory of R.B. Tesh	TVP-1140
Chemicals, Peptides, and Recombinant Proteins		
Streptavidin-HRP	Jackson ImmunoResearch	Cat#016-030-084
Neutravidin	ThermoScientific	Cat#31000
Poly-L-lysine solution	Sigma-Aldrich	Cat#P4707
Medium 199	Lonza	Cat#12-109F
TRIzol-LS	Thermo Fisher Scientific	Cat#10296010
Jeffamine® ED-2001 pH 7.0	Hampton Research	Cat#HR2-597
Fomblin Y oil	Sigma-Aldrich	Cat#317942-100G
Critical Commercial Assays		
Q5 site-directed mutagenesis kit	New England Biolabs	Cat#E0554S
QuikChange site-directed mutagenesis	Agilent Technologies	Cat#200524
Nunc MaxiSorp 384-well ELISA plate	Sigma-Aldrich	Cat#P6491
SuperSignal ELISA Femto Substrate	Thermo Fisher Scientific	Cat#37075
Qiaamp viral RNA mini kit	QIAGEN	Cat#1020953
QIAGEN One-Step RT-PCR	QIAGEN	Cat#210210
Superscript III RT	Thermo Fisher Scientific	Cat#18080093
Nucleospin gel and PCR clean-up	Macherey-Nagel	Cat#740609
Deposited Data		
Z021-ZIKV EDIII structure	This paper	PDB ID: 6DFI
Z021-DENV1 EDIII structure	This paper	PDB ID: 6DFJ
Experimental Models: Cell Lines		
HEK293-6E	National Research Council of Canada	NRC file 11565
Lenti-X 293T	ATCC	Cat#632180; RRID:CVCL_4401
Huh-7.5	Blight et al., 2002	N/A
Vero WHO	Laboratory of S. Whitehead	MCB-P139

(*Continued on next page*)

Continued		
REAGENT or RESOURCE	SOURCE	IDENTIFIER
STAT1$^{-/-}$	Laboratory of J.-L. Casanova, Chapgier et al., 2006	N/A
K-562	ATCC	CAT#:CCL-243; RRID:CVCL_0004
Experimental Models: Organisms/Strains		
Ifnar1$^{-/-}$ mice: B6.129S2-Ifnar$^{1tm1Agt/Mmjax}$	The Jackson Laboratory	JAX stock:32045
Rhesus Macaques (*Macaca mulatta*)	California National Primate Research Center	Breeding colony
Oligonucleotides		
Primers	Table S3 this paper	N/A
Recombinant DNA		
IGγ1-, IGκ or IGλ-expression vectors	Tiller et al., 2008	N/A
pWNVII-Rep-REN-IB	Laboratory of T. Pierson	N/A
pZIKV/HPF/CprME	Laboratory of T. Pierson	N/A
pZIKV/HPF/CprM*E*	Robbiani et al., 2017	N/A
Wild type ZIKV EDIII expression vector	Robbiani et al., 2017	N/A
Software and Algorithms		
Prism (v7)	GraphPad	https://www.graphpad.com
Mosflm (v7.2.1, part of CCP4 package)	Battye et al., 2011	http://www.ccp4.ac.uk
CCP4 (v7.0.032)	Winn et al., 2011	http://www.ccp4.ac.uk
Phenix (v1.11.1-2575)	Adams et al., 2010	http://www.phenix-online.org
Coot (v0.8.7, part of CCP4 package)	Emsley and Cowtan, 2004	http://www.ccp4.ac.uk
AntibodyDatabase (v1.0)	West et al., 2013	N/A
BIAcore T200 evaluation software	GE Healhcare	http://www.biacore.com/lifesciences/index.html
Other		
Biacore T200 SPR system	GE Healthcare	CAT#:28975001
CM5 sensor chip	GE Healthcare	CAT#:BR100399

CONTACT FOR REAGENT AND RESOURCE SHARING

Further information and requests for reagents should be directed to and will be fulfilled by the Lead Contact, Davide Robbiani (drobbiani@rockefeller.edu). Sharing of reagents may require UBMTA agreements.

EXPERIMENTAL MODEL AND SUBJECT DETAILS

Macaques

Rhesus macaques (*Macaca mulatta*) were healthy juveniles or adults from the conventional type D retrovirus-free, SIV-free and simian lymphocyte tropic virus type 1 antibody negative colony at the California National Primate Research Center (CNPRC). All animals were males except for two of the untreated controls (5021 and 5242). Animals were also confirmed to be antibody negative for West Nile virus. Animals were housed in accordance with Association for Assessment and Accreditation of Laboratory Animal Care Standards. We strictly adhered to *Guide for the Care and Use of Laboratory Animals* prepared by the Institute for Laboratory Animal Research. The study was approved by the Institutional Animal Care and Use Committee of the University of California Davis. When necessary for inoculations or sample collections, macaques were immobilized with 10 mg/kg ketamine hydrochloride (Parke-Davis) injected intramuscularly after overnight fasting. Z004 and Z021 antibodies were administered to macaques at doses of 15 mg/kg body weight each by slow intravenous (i.v.) infusion (2ml/minute) 24 hours before saphenous vein i.v. inoculation with Brazilian ZIKV (10^5 PFU in 1 mL of RPMI-1640 medium). Macaques were evaluated twice daily for clinical signs of disease including poor appetence, stool quality, dehydration, diarrhea, and inactivity. None of the animals that received the antibodies developed any clinical signs, suggesting a good safety profile. In contrast, one of four untreated macaques developed a severe transient skin rash in the axillary and inguinal areas on day 6, which peaked on day 8, was treated with topical antibiotics and steroids, and rapidly improved from day 10 onward. Animals were sedated for antibody administration (minus 24h), at time zero (virus inoculation), daily for 7 to 8 days, and then every few days for sample collection. EDTA-anti-coagulated blood samples were collected using venipuncture.

Mice

Interferon-αβ receptor knock-out mice were obtained from The Jackson Laboratory (*Ifnar1*$^{-/-}$; B6.129S2-*Ifnar1*^{tm1Agt}/Mmjax**)** and were bred and maintained in the animal facility at Rockefeller University. Mice were specific pathogen free and on a standard chow diet. Both male and female mice (3-4 week old) were used for experiments and were equally distributed within experimental and control groups. 125 μg of monoclonal antibodies in 200 μL of PBS were administered intraperitoneally to *Ifnar1*$^{-/-}$ mice one day before or one day after footpad infection with 1.25x10^5 plaque forming units (PFU) of ZIKV Puerto Rican strain in 50 μl. Mice were monitored for symptoms and survival over time. Animal protocols were in agreement with NIH guidelines and approved by the Rockefeller University Institutional Animal Care and Use Committee.

Cell lines

Human embryonic kidney HEK293-6E suspension cells were cultured at 37°C in 8% CO_2, shaking at 120 rpm. All other cell lines described below were cultured at 37°C in 5% CO_2, without shaking. Green monkey Vero cells and human hepatocytes Huh-7.5 cells (Blight et al., 2002) were cultured in Dulbecco's Modified Eagle Medium (DMEM) supplemented with 1% nonessential amino acids (NEAA) and 5% FBS. Human Lenti-X 293T cells and STAT1$^{-/-}$, an SV40 large T antigen immortalized skin fibroblast line (Chapgier et al., 2006), were grown in DMEM 10% FBS. K-562 cells were maintained in RPMI supplemented with 10% FBS (ATCC, CCL-243). Huh-7.5 cells were developed in the Laboratory of Virology and Infectious Disease at Rockefeller University and verified by STR (standard tandem repeat). A seed-lot system is in place for these highly utilized cell lines, as well as for other lines obtained from the ATCC. The ATCC implements cell line authentication by STR DNA profiling. STAT1$^{-/-}$ cells are of unknown sex; HEK293-6E, Lenti-X 293T, K-562 and Vero are of female origin; Huh-7.5 are male.

Viruses

For *in vitro* experiments, ZIKV 2015 Puerto Rican PRVABC59 (Lanciotti et al., 2016) was obtained from the CDC and passaged twice in human Huh-7.5 cells, and the Thai isolate of DENV1 PUO-359 (TVP-1140) was obtained from Robert Tesh and amplified by three passages in C6/36 insect cells. For mouse experiments, ZIKV 2015 Puerto Rican PRVABC59 was passaged once in STAT1$^{-/-}$ human fibroblasts. For macaque experiments, a 2015 isolate of ZIKV from Brazil (strain SPH2015; GenBank accession number KU321639.1) was used. The strain was isolated from the plasma of a transfusion recipient and was passaged twice in VERO cells. Virus titrations were performed in African Green Monkey Kidney (VERO) cells using plaque assays. For PRVABC59, 200 μL of 10-fold serial dilutions of virus in OPTI-MEM were used to infect 400,000 cells seeded the previous day in a 6-well format. After 90 minutes adsorption, the cells were overlayed with DMEM containing 2% FBS with 1.2% Avicel and Penicilin/Streptomycin. Four days later the cells were fixed with 3.5% formaldehyde and stained with crystal violet for plaque enumeration. For SPH2015, 250 μL of 10-fold serial dilutions of samples in DMEM were inoculated onto confluent cell monolayers in duplicate in 6-well plates. After 60 minutes adsorption at 37°C, the cells were overlayed with MEM containing 2% FBS with 1.0% Penicilin/Streptomycin in 0.8% agar (liquefied 10% agar, ultrapure agarose [Invitrogen] diluted in 42°C MEM) and allowed to solidify, and incubated at 37°C with 5% carbon dioxide for 8 days. Cell monolayers were then fixed with 4% formalin for 30 minutes, agar plugs were removed, and 0.025% gentian violet (Sigma) in 30% ethanol was overlaid in each well to stain viable cells. Viral titers were recorded as the reciprocal of the highest dilution where plaques are noted. The limit of detection of the assay was 1.6 log10 PFU/ml (Coffey et al., 2017; Robbiani et al., 2017).

METHOD DETAILS

Production of antibodies and Fabs

Z021, Z004, Z015 (Robbiani et al., 2017) and 10-1074 (Mouquet et al., 2012) were prepared by transient transfection of mammalian HEK293-6E cells with equal amounts of immunoglobulin heavy and light chain expression vectors. The supernatant was harvested after seven days and the antibodies purified using Protein G Sepharose 4 Fast Flow. LPS was removed with TritonX-114 and the antibodies concentrated to 4.6 to 19 mg/ml in PBS. The GRLR (Horton et al., 2008; Lu et al., 2016), LS (Ko et al., 2014; Zalevsky et al., 2010) and combined (GRLR/LS) modifications in the Fc portion of Z004 and Z021 human IgG1 expression plasmids (Tiller et al., 2008) were generated with Q5 site-directed mutagenesis kit (New England Biolabs) according to the company's instructions and with the primers listed in Table S3. Fabs expressed for crystallography were expressed by transient transfection of HEK293-6E mammalian cells with equal amounts of C-terminally His-tagged Fab heavy chain (VH-CH1) and light chain expression vectors. The supernatant was harvested after six days and the Fabs were purified by affinity purification using HisTrap HP columns (GE Healthcare Life Sciences). Proteins were eluted with 300mM imidazole and then concentrated and further purified by size exclusion chromatography on a Superdex 200 Increase column (GE Healthcare Life Sciences).

Production of ZIKV proteins

Expression plasmids encoding the ZIKV mutant proteins EDIII$_{E393A/K394A}$, EDIII$_{E393D}$ and EDIII$_{K394R}$ were generated by modifying the wild-type EDIII expression plasmid (Robbiani et al., 2017) using QuikChange site-directed mutagenesis (Agilent Technologies) and confirmed by DNA sequencing. Primers used for mutagenesis are listed in Table S3. Mutant ZIKV EDIII proteins were expressed in *E. coli* BL21(DE3) (New England Biolabs), refolded from inclusion bodies, and purified (Robbiani et al., 2017; Sapparapu et al., 2016). Briefly, upon transformation with an appropriate EDIII protein-encoding expression vector, cells were grown to mid-log phase and

induced with isopropyl β-D-1-thiogalactopyranoside (IPTG) for 4 hours. Upon lysis, the insoluble fraction containing the inclusion bodies was solubilized in buffer containing 6M guanidine hydrochloride, 100mM Tris-HCl pH 8.0, and 20mM β-mercaptoethanol and clarified by centrifugation. The solubilized inclusion bodies were then refolded using rapid dilution into 400 mM L-arginine, 100 mM Tris-HCl (pH 8.0), 2 mM EDTA, and 5 and 0.5 mM reduced and oxidized glutathione at 4°C. The refolded protein was filtered, concentrated, and finally purified by size exclusion chromatography (Superdex 75; GE Healthcare) in 20mM Tris pH 8.0, 150mM NaCl, 0.02% NaN_3.

Generation and production of RVPs

Wild-type ZIKV Reporter Viral Particles (RVPs) with E proteins corresponding to Asian/American or African lineage were previously reported (Robbiani et al., 2017). Plasmids for expression of ZIKV CprME with E mutations were generated from plasmid pZIKV/HPF/CprM*E* (Robbiani et al., 2017), a derivative of pZIKV/HPF/CprME, a ZIKV C-prM-E expression construct provided by Ted Pierson (NIH) and engineered to contain unique *BspHI* and *SacII* restriction sites flanking the envelope region, allowing facile manipulation.

Assembly PCR-based site-directed mutagenesis was used to introduce the E393A-K394A double mutation or K294R single mutation into the envelope of ZIKV H/PF/2013 in pZIKV/HPF/CprM*E*, resulting in plasmids pZIKV/HPF/CprM*E*(E393A-K394A) or pZIKV/HPF/CprM*E*(K294R), respectively. The primers used for assembly PCR and mutagenesis are listed in Table S3. All PCR-derived plasmid regions were verified by sequencing.

RVPs bearing the ZIKV E protein with E393A-K394A or with K294R mutations were generated by cotransfection of Lenti-X-293T cells with plasmids pZIKV/HPF/CprM*E*(E393A-K394A) or pZIKV/HPF/CprM*E*(K294R) with pWNVII-Rep-REN-IB (Pierson et al., 2006; Robbiani et al., 2017). One μg of pWNVII-Rep-REN-IB (WNV replicon expression construct) and 3 μg of the appropriate flavivirus CprME expression plasmid were co-transfected with Lipofectamine 2000 (Invitrogen) according to the manufacturer's instructions. Lipid–DNA complexes were replaced after 4–5 h incubation with DMEM containing 20 mM HEPES and 10% FBS. After 48-72 h incubation at 34°C, RVP-containing supernatants were harvested, filtered through a 0.45 micron filter and frozen at −80°C.

In vitro neutralization and ADE assays

Plaque reduction neutralization test (PRNT) with ZIKV PRVABC59, and flow cytometry-based neutralization assay with DENV1 PUO-359 were used to measure antibody neutralization activity in VERO cells (Robbiani et al., 2017). For ZIKV, diluent medium was Medium 199 (Lonza) supplemented with 1% BSA and Pen/Strep (BA-1 diluent). Briefly, 3- to 10-fold serial human antibody dilutions were added to a constant amount of Huh-7.5-ZIKV stock diluted in BA-1 diluent and incubated for 1 h at 37°C prior to application to VERO cells seeded at 400,000 cells per 6-well the day prior. After 90 minutes adsorption, the cells were overlayed with DMEM containing 2% FBS with 1.2% Avicel and Pen/Strep. Four days later the cells were fixed with 3.5% formaldehyde and stained with crystal violet for plaque enumeration. $PRNT_{50}$ values were determined as the antibody concentration that resulted in 50% of the number of plaques obtained with the no antibody control. For DENV1, 5,000 VERO cells were seeded in 96-well plates. The next day, serial dilutions of antibody were incubated with DENV1 for 1 hr at 37°C and applied to the cells (MOI = 0.02). After 3 days, the cells were fixed with 2% formaldehyde and stained with the pan flavivirus anti-E protein 4G2 monoclonal antibody (2 μg/ml) in PBS containing 1% FBS and 0.5% saponin. Bound antibody was detected with Alexa Fluor 488-conjugated anti-mouse IgG antibody (1:1,000, Invitrogen) and the percentage of infected cells determined by flow cytometry. Percentages of cells infected with DENV1 in the presence of the different concentrations of antibody compared to cells infected with DENV1 in the absence of antibody was used to estimate the 50% reduction.

Neutralization of luciferase-encoding RVPs by antibodies using the ZIKV wild-type, E393A-K394A, K294R, and African mutant RVPs was performed with Huh-7.5 cells. 15,000 cells were seeded in each well of a 96-well plate the day before infection in a volume of 100 μl. RVPs were diluted in BA-diluent, and 100 μL were added to 100 μL of triplicate samples of 3- or 10-fold serially diluted human antibody. After incubation for 1 h at 37°C, 100 μL of the RVP/antibody mixture was added to the cells. After 24 h incubation at 37°C, the medium was removed and cells were lysed in 75 μL lysis buffer and 20 μL used for Renilla luciferase measurement using the Renilla Luciferase Assay System (Promega) according to the manufacturer's instructions and read using a FLUOstar Omega luminometer (BMG LabTech). Neutralization capacity of the antibody was determined by the percentage of luciferase activity obtained relative to activity from RVPs incubated with BA-diluent alone (no antibody). Antibody dependent enhancement (ADE) of infection assays using antibodies or macaque plasma were similar to neutralization assays with RVPs, except that Fc-receptor bearing K-562 cells were used, and that the cells were in 96-well plates coated with 0.01% poly-L-lysine (Sigma). The macaque plasma was serially diluted 1:3 in BA-1 medium (1:50 – 1:328050, 9 dilutions in total). BA-1 medium is Medium 199 (Lonza, 12-109F) supplemented with 1% BSA, 1400 mg/L sodium bicarbonate and 100 U/ml Pen/Strep. The luciferase signal was normalized to the signal obtained with 10ng/ml of antibody Z004, which was present on the same plate.

ELISA assays

Fab ELISA

Figure 1D. 5 μg/mL ZIKV EDIII antigen ($EDIII_{wild\text{-}type}$, $EDIII_{E393A/K394A}$, $EDIII_{E393D}$ or $EDIII_{K394R}$) was adsorbed to a Nunc MaxiSorp 384-well ELISA plate overnight at 4°C. The ELISA plate was blocked with 3% BSA in TRIS buffered saline with 0.05% Tween-20 (TBS–T),

washed with TBS-T, and then serial dilutions of Fab were added and incubated for 3 hours at room temperature. After washing the plate with TBS-T, bound Fab was detected using goat-anti-human IgG-HRP (GenScript; 1 hour, room temperature) and developed with SuperSignal ELISA Femto Substrate (Thermo Fisher).

Antigen competition ELISA

Figure 2G. Serial dilutions of Z004 or Z021 antibody were incubated overnight with nutation at 4°C in V-bottom 96-well plates in the presence of saturating concentrations of either wild-type EDIII, $EDIII_{E393A/K394A}$, or no protein control. In preliminary experiments, the saturating concentration of EDIII protein was determined as being approximately 1 μg/ml, and was increased to 10 μg/ml for the actual experiment. After overnight incubation the samples were added to ELISA plates that had been pre-coated with wild-type EDIII and the residual antibody binding to EDIII was detected using HRP-conjugated goat anti-human IgG (Jackson ImmunoResearch; 1 hour, room temperature). The signal was enhanced by two amplification steps. First, after incubating with goat anti-human IgG-HRP (Jackson ImmunoResearch; 1 hour, room temperature) and washing with PBS containing Tween-20 0.05%, anti-goat IgG-biotin was added (Jackson ImmunoResearch; 1 hour, room temperature). Second, after washing, streptavidin-HRP was added (Jackson ImmunoResearch; 1 hour, room temperature). After the final washes, the reaction was developed with ABTS substrate (Life Technologies).

Antibody competition ELISA

Figure 2I. Z004 or Z021 IgG (5 μg/mL) was adsorbed overnight at 4°C in a Nunc MaxiSorp 384-well ELISA plate. The ELISA plate was blocked with 3% bovine serum albumin (BSA) in TBS–T, and then 5 μg/mL of ZIKV EDIII was added and incubated for 3 hours at room temperature. The plate was washed with TBS-T to remove excess antigen, and Fab was then added at 25 μg/mL and incubated for 3 hours at room temperature. Bound His-tagged Fab was detected using THE His Tag Antibody (Genscript; 1 hour, room temperature), followed by goat-anti mouse IgG-HRP (Jackson ImmunoResearch; 1 hour, room temperature), and developed with SuperSignal ELISA Femto Substrate (Thermo Fisher). Relative light units were plotted for each IgG-antigen pair.

ELISA for human IgG detection in macaque

Figure S2. Neutravidin (ThermoScientific; 2 μg/ml in PBS) was absorbed to high binding 96-well plates for overnight at 4°C. After washing the plate using PBS with 0.05% Tween-20 (PBS-T), the biotinylated anti-human IgG capture antibody was added (ThermoScientific; 2 mg/ml in PBS-T, 1 hour at room temperature). Upon washes, the plates were blocked with 2% BSA in PBS-T (2 hours at room temperature), blotted, and then serial dilutions of the macaque plasma were added to the wells (5 steps of 1:4 dilutions in PBS-T, starting with 1:10). Each plate included serial dilutions of the standard, in duplicates (Z004 IgG, 11 steps of 1:3 dilutions in PBS-T, starting with 10 μg/ml). Plates were incubated for 1 hour at room temperature and washed prior to adding the detection reagent anti-human IgG-HRP (Jackson Immunoresearch; 1 hour at room temperature). After the final washes, the reaction was developed with ABTS substrate (Life Technologies).

Surface plasmon resonance

FcγR and FcRn binding affinity of the Z004 Fc domain variants was determined by surface plasmon resonance (SPR) (Li et al., 2017; Wang et al., 2017b). Briefly, all experiments were performed on a Biacore T200 SPR system (GE Healthcare) at 25°C in HBS-EP^+ buffer (GE Healthcare; pH 7.4 for FcγRs, pH 6.0 for FcRn). Recombinant protein G (Thermo Fisher) was immobilized to the surface of a CM5 sensor chip (GE Healthcare) using amine coupling chemistry at a density of 500 resonance units (RU). Fc variants of the Z004 antibody were captured on the Protein G-coupled surface (250 nM injected for 60 s at 20 μl/min) and recombinant human FcγR ectodomains (7.8125 – 2000 nM; Sinobiological) or FcRn/β2 microglobulin (1.95 – 500 nM; Sinobiological) were injected through flow cells at a flow rate of 20 μl/min. Association time was 60 s followed by a 600 s dissociation step. At the end of each cycle, the sensor surface was regenerated with 10 mM glycine, pH 2.0 (50 μl/min; 40 s). Background binding to blank immobilized flow cells was subtracted and affinity constants were calculated using BIAcore T200 evaluation software (GE Healthcare) using the 1:1 Langmuir binding model.

Processing of macaque blood samples

EDTA-anticoagulated blood was processed immediately by centrifugation for 10 minutes at 800 X g to separate plasma from cells. The plasma was spun an additional 10 minutes at 800 X g to further remove cells, and aliquots were immediately frozen at −80°C. The cellular blood fraction was diluted with PBS and layered on lymphocyte separation medium (MP Biomedicals) and spun for 30 m at 800 g to isolate peripheral blood mononuclear cells that were washed and then cryopreserved for future analyses. Complete blood counts (CBC) were performed on EDTA-anticoagulated blood samples; samples were analyzed using a Pentra 60C+ analyzer (ABX Diagnostics); differential counts were determined manually using Wright-Giemsa staining.

Isolation and quantitation of viral RNA

Zika virus RNA was isolated from plasma and measured by RT-qPCR according to methods described previously (Lanciotti et al., 2008) and detailed below, which were modified to increase the initial volume of sample tested from 140 to 300 μL (when available) to increase sensitivity. RNA was extracted from plasma according to manufacturer's recommendations using an Applied Biosystems MagMax 96-well Viral RNA kit and the AM1836 DW200 STD program on a MagMax Express 96-Deep Well Magnetic Particle Processor (ThermoFisher, Waltham, MA). All RNA extracts were eluted in 60 μL of DEPC-treated water for storage at −80°C prior to quantification. ZIKV RNA was measured in triplicate by reverse transcription RT-qPCR on an Applied Biosystems ViiA 7 machine

using the Taqman Fast Virus 1-Step Master Mix (Thermo) and published primers (ZIKV 1086, ZIKV 1162c, and ZIKV 1107-FAM; (Lanciotti et al., 2008)) with 9.6 μL of RNA. Levels of ZIKV RNA in samples are expressed as mean $\log_{10}$ copies per ml plasma.

Virus sequencing

For detection of virus escape mutations in macaques, ZIKV RNA was extracted at peak viremia from plasma using the Qiaamp viral RNA mini kit following the manufacturer's recommendations with elution of RNA in water. QIAGEN One-Step RT-PCR was performed using either of two primer sets targeting sequences surrounding the ZIKV EDIII region (see Table S3), with 50°C for 30 m, 95°C for 15 m. Next, 40 cycles of each of the 3 steps were performed: 94°C for 1 m, 58°C for 1 m, 72°C for 1m15s, followed by final extension of 72°C for 10 m. RT-PCR amplicons were visualized on 1% agarose gels stained with ethidium bromide and sequenced after purification using the Qiaquick PCR purification kit. Sequences were called based on clean chromatograms sequenced with the primers used for amplification. Due to very low levels of viremia, reliable EDIII sequence information was obtained for only 210 out of 303 nucleotides from macaque 6082 (Z004+Z021), and no sequencing was possible from macaque 6146 (Z004+Z021 GRLR). Viral sequences in mice were from blood. RNA was extracted from TRIzol-LS (Life Technologies) and reverse transcribed with Superscript III RT (Thermo Fisher Scientific) and random primers according to the company's protocol prior to PCR amplification of the ZIKV EDIII region with primers DFRp1284 and DFRp1469 followed by PCR clean-up with Nucleospin (Macherey-Nagel) and direct sequencing with primer DFRp1283. Where necessary, a second round of nested PCR was performed with primers DFRp1472 and DFRp1470. The primers sequence is listed in Table S3.

Crystallization and structure determination

Z021-ZIKV EDIII complex

The complex for crystallization was produced by mixing Z021 Fab and ZIKV EDIII at a 1:1 molar ratio, incubating at room temperature for 1-2 hours, and concentrating to 14.1 mg/mL. Crystals of Z021 Fab–ZIKV EDIII complex (space group $P2_12_12_1$; a = 73.88 Å, b = 105.62 Å, c = 107.24 Å; one molecule per asymmetric unit) were obtained by combining 0.2 μL of protein complex with 0.2 μL of 0.1M HEPES pH 7.0, 29% PEG 1000 in sitting drops at 22°C. Crystals were cryoprotected with 25% glycerol.

X-ray diffraction data were collected at Advanced Photon Source (APS) beamline 23-ID-D using a Dectris Pilatus 6M detector. The data were integrated using Mosflm (Battye et al., 2011) and scaled using CCP4 (Winn et al., 2011). The Z021-ZIKV EDIII complex structure was solved by molecular replacement using the V_HV_L and C_HC_L domains from our Z021-DENV1 EDIII complex and ZIKV EDIII from PDB 5KVG as search models in Phenix (Adams et al., 2010). The model was refined to 2.48 Å resolution using an iterative approach involving refinement in Phenix and manual rebuilding into a simulated annealing composite omit map using Coot (Emsley and Cowtan, 2004). The final model (R_{work} = 18.2%; R_{free} = 22.8%) contains 537 protein residues and 68 water molecules. 96%, 4%, and 0.2% of the protein residues were in the favored, allowed, and outlier regions, respectively, of the Ramachandran plot. Residues that are disordered and not included in the model are: HC residues 216-219 and the 6X His tag; LC residue 214, and ZIKV EDIII residues 299-302 and 405-407. The accession number for the Z021-ZIKV EDIII complex crystal structure reported in this paper is PDB: 6DFI.

Z021-DENV1 EDIII complex

The complex for crystallization was produced by mixing Z021 Fab and DENV1 EDIII at a 1:1 molar ratio, incubating at room temperature for 1-2 hours, and concentrating to 12.25 mg/mL. Crystals of Z021 Fab–DENV1 EDIII complex (space group $C222_1$; a = 60.54 Å, b = 91.60 Å, c = 187.14 Å; one molecule per asymmetric unit) were obtained by combining 0.2 μL of protein complex with 0.2 μL of 0.1M sodium citrate pH 4.8, 28% Jeffamine® ED-2001 pH 7.0 in sitting drops at 22°C. Crystals were cryoprotected with Fomblin Y oil.

X-ray diffraction data were collected at Stanford Synchrotron Radiation Lightsource (SSRL) beamline 12-2 using a Dectris Pilatus 6M detector. The data were integrated using Mosflm (Battye et al., 2011) and scaled using CCP4 (Winn et al., 2011). The Z021-DENV1 EDIII complex structure was solved by molecular replacement using the V_HV_L and C_HC_L domains from PDB 4YK4 and DENV1 EDIII from PDB 4L5F as search models in Phenix (Adams et al., 2010). The model was refined to 2.07 Å resolution using an iterative approach involving refinement in Phenix and manual rebuilding into a simulated annealing composite omit map using Coot (Emsley and Cowtan, 2004). The final model (R_{work} = 18.4%; R_{free} = 23.2%) contains 532 protein residues and 126 water molecules. 96%, 4%, and 0% of the protein residues were in the favored, allowed, and disallowed regions, respectively, of the Ramachandran plot. Residues that are disordered and not included in the model are: HC residues 215-219 and the 6X His tag; LC residues 213-214. The Z021-DENV1 EDIII complex crystal structure has been deposited in the Protein Data Bank with accession code PDB: 6DFJ.

QUANTIFICATION AND STATISTICAL ANALYSIS

Information on the statistical tests used, and the exact values of n and what it represents can be found in the Results and Figure Legends. Unless otherwise noted, statistical analysis was with Prism software. Luciferase- and flow cytometry-based neutralization and enhancement assays were performed in triplicate wells, and the antibody concentration (IC_{50}) that neutralized 50% of the virus or RVP inoculum was calculated by nonlinear, dose-response regression analysis. Representatives of at least two independent experiments are shown throughout, except for ZIKV neutralization (where the mean of two experiments is shown), and for the measurement of ADE in macaque plasma (where only one assay was performed due to limited amounts of available plasma). The levels of plasma viremia were measured in triplicates. The Mantel-Cox test was applied to analyze disease

and survival in mice infection experiments and the Mann-Whitney test to determine the significance of the difference in peak viremia in macaques.

DATA AND SOFTWARE AVAILABILITY

The accession numbers for the structural data reported in this paper are PDB: 6DFI (Z021-ZIKV EDIII complex) and PDB: 6DFJ (Z021-DENV1 EDIII complex).